Journal of Inclusion Phenomena and Macrocyclic Chemistry

Original Article

Title: Examination of the physicochemical properties of caffeic acid complexed with γ-cyclodextrin

Yutaka Inoue, Kengo Suzuki, Toshinari Ezawa, Isamu Murata, Mami Yokota, Yoshihiro Tokudome, Ikuo Kanamoto

*To whom correspondence should be addressed:

Yutaka Inoue

Faculty of Pharmaceutical Sciences, Josai University

1-1 Keyakidai, Sakado-shi, Saitama, 3500295, Japan

Tel: +81-49-271-7317

Fax: +81-49-271-7317

E-mail: yinoue@josai.ac.jp

Abstract

Caffeic acid (CA) is a hydrophobic polyphenol with a high antioxidant capacity and γ-cyclodextrin (γ-CD) is a cyclic polysaccharide. The current study prepared a coprecipitate (CP), a freeze-dried (FD) preparation, a ground mixture (GM), and a physical mixture (PM) of CA and γ-CD, and this study then assessed the physicochemical properties and antioxidant capacity of these preparations. PXRD patterns revealed that a PM and a GM prepared at a certain molar ratio (CA/γ-CD =1/1) produced a diffraction peak due to CA crystals. Diffractions peaks characteristic of CA and γ-CD disappeared with the CP, but new peaks were noted. In addition, an FD with CA and γ-CD at a molar ratio of 1/1 produced a halo pattern. DSC measurements revealed that the PM produced an endothermic peak at 220 ^{o}C due to the melting of CA, but the endothermic peak due to CA disappeared with the CP, FD, and GM. IR spectra revealed that the absorption peak due to the carbonyl group (C=O) of CA shifted for both the CP and the FD. The absorption peak due to C=C in the aromatic ring of CA also shifted. These findings presumably indicate molecular interaction between CA and γ-CD when the 2 substances are present at a molar ratio of 1/1 (CA/γ-CD). In the GM, molecular interaction presumably occurred as a result of heat. The preparations were compared to CA alone in dissolution testing, which revealed that the CP and FD both had a high rate of dissolution. ^{1}H-^{1}H NMR (NOESY) spectra revealed cross peaks involving protons of the γ-CD cavity and protons of the aromatic ring of CA. Thus, the formation of CA and γ-CD inclusion complexes helped to improve the dissolution of CA and γ-CD at a molar ratio of 1/1. The CP and FD had a higher antioxidant capacity than did CA alone. This presumably indicates that the formation of CA and γ-CD inclusion complexes helped to increase the electron density of CA in the CD cavity.

Keywords: caffeic acid, cyclodextrin, inclusion complex, physicochemical property, antioxidant

Introduction

Over the past few years, the prevalence of lifestyle-related diseases such as hypertension, diabetes, and hyperlipidemia has increased [1]. However, health consciousness is more prominent than ever before, and there is an increasing interest in foods with nutrient function claims. Catechin, for example, is an astringent ingredient in green tea and may be effective at preventing lifestyle-related diseases because of its various biological activities [2]. Like catechin, caffeic acid (CA) is also a polyphenol, although CA is found in coffee.

CA is a hydrophobic polyphenol with a high antioxidant capacity because it has a catechol structure on the phenolic ring and because it has a double bond conjugated with the catechol structure [3-4]. Substances with a high antioxidant capacity protect cells by preventing oxidative cell damage through the suppression of active oxygen. In addition, those substances are reported to exhibit anti-inflammatory action by reducing inflammatory cytokines [5]. Those substances are also thought to selectively induce apoptosis in cancer cells and to inhibit the invasion of cancer cells [6]. Since CA has a high antioxidant capacity and various biological activities, it has garnered attention over the past few years. However, CA has a low bioavailability when orally administered because of its low solubility in water, slowing the rate of its absorption. As a result, the level of CA in the blood does not increase, preventing CA from being sufficiently effective.

Cyclodextrins (CDs) contain glucopyranose units linked with α-1,4-glucosidic bonds. Because of these bonds, CDs form a cyclic structure shaped like a truncated cone with an internal cavity. The cavity is hydrophobic while the outer ring is hydrophilic. Thus, CDs are known to form inclusion complexes since various hydrophobic guest molecules can be encapsulated in the cavity, such as by hydrophobic interaction in an aqueous solution [7-8]. γ-cyclodextrin (γ-CD) is a ring-shaped molecule consisting of 8 glucose units linked by α-1,4-glucosidic bonds. The Joint FAO/WHO Expert Committee on Food Additives (JECFA)

has allocated an acceptable daily intake (ADI) of "not specified" to γ-CD (this is the most desirable ADI allocation issued by the JECFA). γ-CD is known to form inclusion complexes and is safely consumed in water-soluble form. CD inclusion complexes are prepared in a variety of ways, such as co-precipitation [9], kneading [10], freeze-drying [11], and co-grinding [12]. Differences in the method of preparation are reported to result in different forms of inclusion. Different forms of inclusion result in CD crystals with different structures, and this leads to differences in solubility even though complexes contain the same host and guest molecules [13]. For example, inclusion complexes of budesonide and γ-CD have a crystal structure with a tetragonal or hexagonal form; the tetragonal form is reported to have greater distance between molecules and thus dissolve faster [14]. The formation of inclusion complexes is reported to improve the solubility of guest molecules in water. The solubility of prostaglandin E2 has been improved by forming prostaglandin E2/αCD inclusion complexes, and formulations containing these complexes are in clinical use [15]. Encapsulating a guest molecule within the CD cavity serves to protect the guest molecule from environmental factors, resulting in increased stability during exposure to oxygen, heat, and light [16]. Drugs that are taken orally must pass through the lipid bilayer membrane of cells to be absorbed in the digestive tract. Thus, drugs must be sufficiently lipid-soluble (hydrophobic) to pass through the cell membrane, but the drug must also be sufficiently water-soluble (hydrophilic) since digestive fluids in the gastrointestinal tract mostly consist of water. Thus, drugs that are highly hydrophilic will dissolve too early, presenting a dilemma. CDs can improve solubility in water by encapsulating a hydrophobic guest molecule, thereby resulting in improved bioavailability [17]. Furthermore, substances with conjugated double bonds exhibit radical-scavenging ability. When CD forms an inclusion complex with a guest molecule, the electron density in the guest molecule shifts, resulting in a complex with improved antioxidant activity [18]. Thus, supramolecular synthesis has been used to alter the solubility, stability, bioavailability, and antioxidant capacity of substances in the presence of CD,

resulting in improved physicochemical properties and biological activity.

A solvent is typically used in freeze-drying and co-precipitation, but the current study formed inclusion complexes of CA and γ-CD by mixing the two into physical mixtures and ground mixtures without using such a solvent. The physicochemical properties of the preparations and their forms of inclusion were studied. CA/γ-CD inclusion complexes were formed in an attempt to improve their solubility in water and antioxidant capacity.

Experimental

Materials and methods

Materials

γ-CD was provided by Wacker Corporation and stored at a temperature of 40 ^{o}C and RH of 82% for 7 days. Caffeic acid (CA) was purchased from Tokyo Kasei Co., Ltd (Fig.1). 2,2-diphenyl-1-picrylhydrazyl (DPPH) was purchased from Sigma-Aldrich Co., LLC. All other reagents were of analytical grade and were purchased from Wako Pure Chemical Industries, Ltd.

Preparation of samples

A physical mixture (PM) was prepared by mixing CA and γ-CD with a vortex mixer for 1 minute at molar ratio of 1/1 (CA/γ-CD). A ground mixture (GM) was prepared by grinding the PM (1.0 g) using a vibrating rod mill (TI-500ET, CMT Co.) with an aluminum pan. A coprecipitate (CP) was prepared by drop-wise addition of an aqueous solution of γ-CD (0.1 M) in 5 mL of methanol (0.1M) to 5 mL of CA. The solution was stirred for 24 hours at room temperature and then allowed to stand at room temperature for 24 hours. The sample was

filtered with filter paper. The precipitate was washed with 5 mL of methanol and vacuum-dried in a desiccator for 24 hours [9]. A freeze-dried (FD) preparation was prepared with CA at a concentration of 20 μg/mL. An aqueous solution of CA and γ-CD at various molar ratios was first prepared and then temporarily frozen at -30 °C. The frozen mixture was freeze-dried using a vacuum freeze dryer (FZ-6, ALS Co., Ltd.).

Powder x-ray diffraction (PXRD)

The PXRD patterns of the samples were measured using an x-ray diffractometer (MiniFlex Ⅱ, Rigaku) with Cu Kα radiation, a voltage of 30 kV, a current of 15 mA, a scan range of 5-30°, and a scan rate of 4°/min.

Differential scanning calorimetry (DSC)

The thermal behavior of the samples was recorded using a differential scanning calorimeter (Thermo plus Evo, Rigaku) with a nitrogen flow rate of 60 mL/min and a heating rate of 5.0 °C/min from 35 to 260 °C.

Fourier transform infrared (FT-IR) spectroscopy

The FT-IR absorption spectra of samples were recorded using a spectrometer (FT/IR-410, JASCO) based on the KBr disk method. Scanning was performed over a range of 650-4,000 cm^{-1} with a resolution of 4 cm^{-1}.

Scanning electron microscopy (SEM)

SEM was performed using a S3000N Scanning Electron Microscope (Hitachi High-Technologies Corporation) at an acceleration voltage of 15 kV. Solvent evaporation time was 70 s. Prior to examination, samples were mounted on aluminum SEM stubs using adhesive tape and then coated with a layer of gold to make them electrically conductive.

Measurement of ^{1}H- nuclear magnetic resonance (NMR) spectra

The ^{1}H NMR spectra (1D) of the samples were measured using an NMR spectrometer (Varian NMR System 400, Agilent) with a D_2O solution. The measurement conditions were as follows: a pulse width of 90°, a relaxation delay of 6.4 μs, a scan time of 3.723 s, and a temperature of 295 K.

The molar ratio of CA to γ-CD was calculated using the following equation (1):

$$X = Y / 8 \quad \ldots(1)$$

X: The number of γ-CD molecules with respect to 1 CA molecule

Y: Integrated intensity of the H-1 in the γ-CD

Measurement of ^{1}H-^{1}H nuclear Overhauser effect spectroscopy (NOESY) NMR spectra

^{1}H-^{1}H NOESY NMR spectroscopy and selective 1D NMR spectroscopy were performed using an NMR spectrometer (Varian NMR System 700NB, Agilent) with a cold probe operating at 699.7 MHz and a D_2O solution. The measurement conditions were as follows: a pulse width of 90°, an acquisition time of 7.0 μs, a relaxation delay of 0.267 s, a mixing time of 4.500 s, a fixed delay of 1.500 s, and a temperature of 298 K.

Dissolution profile

Dissolution testing of the samples was performed using a dissolution apparatus (NRT-593, Toyama Sangyo Co., Ltd.) at 37±0.5 °C with 900 mL of distilled water, which was stirred at 50 rpm using the paddle method. The samples were weighed accurately and equivalent to 100 mg of CA. Twenty 20 mL of the dissolved sample was collected at 5, 10, 15, 30, 60, 90, and 120 min and filtered through a 0.45-μm membrane filter. An equal volume of fresh dissolution medium, maintained at the same temperature, was added after the withdrawal of each sample to keep the volume of dissolution medium constant.

Quantification was performed using a Waters e2795 ultraviolet-visible spectrophotometer (Nippon Waters Co., Ltd.) at a wavelength of 285 nm. An Inertsil®ODS-3 column (φ5 μm, 150 mm × 4 mm) (GL Sciences Inc.) was used. The sample injection volume was 30 μL and the column temperature was 40 °C. A mixture of distilled water / acetonitrile / methanol / acetic acid (99.7%) (862/113/20/5) was used as a mobile phase and the retention time of CA was set at 10 min.

DPPH radical scavenging test

Radical scavenging was measured using a Spectra Max 190 Microplate reader (Molecular Devices Japan Co., Ltd.). A DPPH methanolic solution and 100 μM of each sample were mixed in a microplate at a ratio of 1/1 (by volume). The mixture was then incubated at 25 °C for 5 min and shielded from light. The absorbance of DPPH was measured at a wavelength of 517 nm. A mixture of DPPH / water (1/1) with a rate of radical removal of 0% (A0) and a mixture of methanol / water (1/1) with a rate of radical removal of 100% (Br) were prepared. The concentration of γ-CD alone was the concentration of γ-CD with respect to the concentration of CA when the two were mixed at a molar ratio of 1/1.

The rate of DPPH radical-scavenging activity (RSA) was calculated using the following formula [18]:

$$\text{Radical-scavenging activity} = [1-(Ab_s\text{-Blank})/(Ab_0\text{-Blank})] \times 100 \quad \ldots(2)$$

Ascorbic acid (AA) is known to generally have a high antioxidant capacity, so AA at the same concentration as CA was used for comparison.

Results and Discussion

PXRD patterns revealed the disappearance of diffraction peaks characteristic of CA in the CP and FD. Results of thermal analysis using DSC revealed the disappearance of an endothermic peak due to the melting of CA in the CP and FD. ^{1}H-^{1}H NOESY NMR spectra revealed cross peaks for the CP and FD, suggesting that CA/γ-CD inclusion complexes were formed. The formation of inclusion complexes with γ-CD helped to increase the solubility of CA and increase its antioxidant capacity.

Examination of the crystalline state

PXRD patterns revealed that CA alone produced a diffraction peak at $2\theta=26.9^{o}$ (Fig. 2-a). γ-CD alone produced a diffraction peak at $2\theta=14.1^{o}$ (Fig. 2-d). The strongest diffraction peak produced by γ-CD was a characteristic peak at $2\theta=22.4^{o}$. With the PM, a diffraction peak at $2\theta=14.1^{o}$ due to γ-CD and a diffraction peak at $2\theta=26.9^{o}$ due to CA were noted (Fig. 2-g). Thus, diffraction peaks for CA alone and γ-CD alone remained, so 2 types of crystals were presumably present. With the CP, diffraction peaks due to CA and due to γ-CD disappeared, and new diffraction peaks at $2\theta=7.5^{o}$, 12.0^{o}, and 16.5^{o} were noted (Fig. 2-h). This is because inclusion complexes were formed, resulting in the disappearance of diffraction peaks characteristic of CA and γ-CD. Instead, new peaks ($2\theta=7.5^{o}$, 12.0^{o}, 16.5^{o}), i.e. diffraction peaks specific to inclusion complexes of γ-CD and a guest molecule, were noted [19]. With the FD, the characteristic diffraction peaks disappeared, and a halo pattern was produced (Fig. 3-i). In the FD, CA forms inclusion complexes with γ-CD in an aqueous solution, disrupting the regularity of the crystal lattice of CA and decreasing the crystallinity of CA. This is presumably why a broad peak, i.e. a halo pattern, due to γ-CD was noted. In the GM, mechanochemical action resulted in molecular interaction between CA and γ-CD. A diffraction peak due to CA crystals disappeared, and only a slight diffraction peak due to inclusion complexes was noted.

Examination of thermal properties

DSC measurements revealed that CA alone had an endothermic peak at 222 °C due to the melting of CA (Fig. 3-a). The PM produced a peak due to the melting of CA at 222 °C, so only CA crystals were present (Fig. 3-c). With the CP, disappearance of the endothermic peak due to CA was noted (Fig. 3-d). PXRD patterns revealed that the CP produced diffraction peaks due to inclusion complexes. Thus, CA forms inclusion complexes with γ-CD, resulting in the disappearance of CA crystals and the disappearance of the endothermic peak due to the melting of CA [20]. With the FD and GM, the endothermic peak due to CA disappeared (Fig. 3-e, f), suggesting the formation of inclusion complexes as occurred in the CP. With the GM, disappearance of the endothermic peak due to CA was noted (Fig. 3-f). PXRD patterns from the GM suggested that some CA and γ-CD molecules formed inclusion complexes as a result of co-grinding. The disappearance of the endothermic peak due to CA may have been caused by the remaining CA and γ-CA molecules forming inclusion complexes as a result of heat [21]. Thus, the endothermic peak due to CA disappeared.

Examination of molecular states in solids

IR spectroscopy was performed to ascertain the state of CA and γ-CD molecules in solids. IR spectra revealed that CA alone produced a peak at 3433 cm^{-1} due to the hydroxyl groups (-OH) of CA. In addition, a peak at 1644 cm^{-1} due to the ester group of CA and a peak at 1619 cm^{-1} due to C=C in the aromatic ring of CA were noted (Fig. 4-a)[22]. The PM produced a peak at 3433 cm^{-1} due to the OH groups of CA, a peak at 1644 cm^{-1} due to the carboxyl group of CA, and a peak at 1599 cm^{-1} due to the aromatic ring (C=C) of CA (Fig. 4-c). The CP and FD produced broad peaks from 3000 cm^{-1} to 3700 cm^{-1} due to hydroxyl groups (-OH). In addition, the peak at 1644 cm^{-1} due to the carboxyl group (C=O) of CA shifted to 1687 cm^{-1}, and the peak at 1599 cm^{-1} due to C=C in the aromatic ring shifted to 1608 cm^{-1} (Fig. 4-d,e).

Peaks produced by hydroxyl groups broadened because CA and γ-CD formed inclusion complexes, producing hydrogen bonds between the OH groups of CA and the γ-CD cavity. In addition, peaks due to the carboxyl group (C=O) and aromatic ring (C=C) of CA shifted. Thus, there was molecular interaction between CA and γ-CD in a solid state. The GM produced broad peaks from 3000 cm^{-1} to 3700 cm^{-1} due to hydroxyl groups (-OH), and the peak due to the carboxyl group of CA shifted to 1684 cm^{-1}. CA alone produced a peak at 1644 cm^{-1} due to the carboxyl group of CA and a peak at 1599 cm^{-1} due to the aromatic ring of CA. These peaks were also noted with the GM (Fig. 4-f). Thus, there were some solitary CA molecules that presumably did not interact with γ-CD in the GM.

Examination of the shape of granules

SEM findings indicated that CA and γ-CD alone both had a smooth surface, and both had granules that were about 50 μm in size (Fig. 5-a,d). Freeze-drying produced needle-shaped granules of CA. In addition, the FD had smaller granules than CA alone (Fig. 5-b). Grinding CA alone produced smaller granules that clung to a larger granule (Fig. 5-c). Freeze-drying of γ-CD produced granules with occasional pitting in an otherwise smooth surface (Fig. 5-d). Grinding γ-CD produced rock-like granules with a rough surface (Fig. 5-f). Changes in the texture of the granule surface or in the size of granules were not noted in the PM (Fig. 5-g). The CP had clumps of small granules, and these granules had a rougher surface than that of granules in the other samples (Fig. 5-h). The FD had granules with a smooth surface, and small granules were packed into clumps about 10 μm in size (Fig. 5-i). The GM had granules with a surface that was rougher than that noted with CA or γ-CD alone (Fig. 5-j). Changes in the texture of the granule surface are characteristically noted when inclusion complexes are formed [23]. The texture of the granule surface differed markedly for the CP, FD, and GM in comparison to CA and γ-CD alone. These findings suggested that CA and γ-CD molecules may form inclusion complexes in a solid state.

Examination of molecular states in solution

The molar ratio of CA and γ-CD in the CP was determined based on ^{1}H NMR spectroscopy. The ratio of the integrated intensity of H-a of CA (Fig. 1) and the integrated intensity of H-1 of γ-CD (Fig. 1) was calculated. The integrated intensity of H-1 of γ-CD was approximately 9.44 with respect to an integrated intensity of H-a of CA of 1 (Fig. 6). γ-CD has a structure with 8 D-glucopyranose units linked to one another in a ring, so about 1 γ-CD molecule is present with respect to each CA molecule. This suggested that inclusion complexes in the coprecipitate had a molar ratio of 1/1 (CA/γ-CD).

X=Y/8

X: The number of γ-CD molecules with respect to 1 CA molecule

Y: Integrated intensity of the H-1 in γ-CD

Use of ^{1}H-^{1}H NOESY NMR spectroscopy to assess molecular interaction

^{1}H-^{1}H NOESY NMR spectra revealed cross peaks involving the protons H-3, H-5, and H-6 in the γ-CD cavity and the protons H-c, H-d, and H-e of the phenolic ring of CA and the protons H-a and H-b of the vinylene group of CA in the CP and FD. Cross peaks involving H-c, H-d, and H-e of the phenolic portion of CA and H-6 of γ-CD had a strong intensity (Fig. 7). These findings presumably suggest that the phenolic ring of the CA molecule is included from the wider to the narrower rim of the ring of γ-CD. Interaction between the protons of the γ-CD cavity and protons of the phenolic ring and vinylene group of CA was noted, so the CA molecule is included in the cavity of the γ-CD molecule, forming an inclusion complex (Diagram. 1). Similar findings were noted with the GM, so solitary CA molecules in an aqueous solution that were not included formed inclusion complexes with solitary γ-CD molecules.

Dissolution test

Dissolution testing indicated that about 70% of CA eluted when CA alone was dissolved for 30 min. The PM had a dissolution profile like that of CA alone. CA crystals were present in the PM, so the PM had poor wetting like that of CA alone. As a result, the dissolution profile of the PM did not change. In contrast, elution of CA was noted in the early stages in the GM, CP, and FD. This is because CA/γ-CD inclusion complexes were formed, so the crystallinity of CA disappeared and CA/γ-CD inclusion complexes resulted in a different crystalline structure. Thus, the poor wetting of CA crystals was remedied and the rate of CA dissolution improved (Fig. 9). Therefore, the formation of CA/γ-CD inclusion complexes helped to improve the rate of CA elution. In the GM, CA and γ-CD molecules that were not included as a result of co-grinding interacted hydrophobically in an aqueous solution. CA and γ-CD formed inclusion complexes, resulting in a dissolution profile similar to that of the FD and CP.

DPPH radical scavenging test

Results of the DPPH radical scavenging test indicated that DPPH radical scavenging by CA alone had a 50% inhibitory concentration (IC_{50}) of 2.57 μg/mL, and this value was similar to the IC_{50} for AA of 2.94 μg/mL. In addition, the IC_{50} for the CP was 2.12 μg/mL and the IC_{50} for the FD was 2.36 μg/mL. These values were significantly smaller than the IC_{50} for AA (Figs. 10 and 11). There are two reasons for this finding. γ-CD itself has moderate antioxidant capacity (Fig. 10), and the electron density increased because of the presence of the CA molecule in the γ-CD molecule. As a result, the CA molecule is more likely to liberate protons and subsequently scavenge DPPH radicals [18].

Conclusion

The current study used coprecipitation and freeze-drying to prepare CA and γ-CD in a solid

state, and this study ascertained molecular interaction between CA and γ-CD based on PXRD patterns, DSC measurements, IR spectra, SEM findings, and ^{1}H-^{1}H NOESY NMR spectra. Results suggested that γ-CD forms inclusion complexes with CA as the guest molecule. These inclusion complexes had a molar ratio of 1/1 (CA/γ-CD). The formation of inclusion complexes results in an improved rate of dissolution that helps to improve the bioavailability of CA. Moreover, the formation of CA/γ-CD inclusion complexes helps to increase the electron density of the CA molecule and it helps CA to inactivate radicals (by making them more stable), thus resulting in increased antioxidant capacity. These findings suggest that the improved dissolution of CA and the increased antioxidant capacity of CA are closely related to its formation of inclusion complexes with γ-CD.

Acknowledgment

The authors wish to thank Cyclo Chem Co. Ltd. for providing γ-CD.

Conflicts of interest

The authors declare no conflicts of interest.

References

1. Christian, E., Thomas, J.D., Susanne, W., Felix, L., Florian B., Nadine W., Maani H., Dittmar, B., Hugo A.K., Christian, A.G.: Expression of IL-17A in human atherosclerotic lesions is associated with increased inflammation and plaque vulnerability. Basic Res. Cardiol. **106**, 125-134 (2011)
2. Tadashi, H., Yumiko, K., Sinichi, M., Yoko, T., Hidekazu, T., Yuji, M., Setsujiro, I., Yoshihisa, K., Ichiro, T., Hiroyuki, S., Hiroshige, I.: Anti-obesity Effects of Tea Catechins in Humans. J. Oleo Sei. **50**, 599-605 (2001)
3. Khushwant, S.B., Grégoire, L., Mohamed, T., Vasantha, R.: Antihypertensive effect of caffeic acid and its analogs through dual renin-angiotensin-aldosterone system inhibition. Eur. J. Pharmacol. **730**, 125-132 (2014)
4. Jiang, H.C., Chi-Tang, H.: Antioxidant Activities of Caffeic Acid and Its Related Hydroxycinnamic Acid Compounds. J. Agric. Food Chem. **45**, 2374-2378 (1997)
5. Monika, M., Stefanie, H., Alois, J.: Anti-inflammatory activity of extracts from fruits, herbs and spices. Food Chemistry. **122**, 987-996 (2010)
6. J,J, Casciari., N,H, Riordan., T,L, Schmidt., X,L, Meng., J,A, Jackson., H,D, Riordan.: Cytotoxicity of ascorbate, lipoic acid, and other antioxidants in hollow fibre in vitro tumours. Br. J. Cancer. **84**, 1544-1550 (2001)
7. Marcus, E.B., Thorsteinn L.: Cyclodextrins as pharmaceutical solubilizers. Adv. Drug. Deliv. Rev. **59**, 645-666 (2007)
8. Tao, T., Yan, Z., Jinjin, W., Beiyi, Z.: Preparation and evaluation of itraconazole dihydrochloride for the solubility and dissolution rate enhancement. Int. J. Pharm. **367**, 109-114 (2009)
9. Mohsen, A., Khalid, A., Abdulaziz, A.: Effect of inclusion complexation with cyclodextrins on photostability of nifedipine in solid state. Int. J. Pharm. **243**, 107-117 (2002)

10. Arumugam, S.P., Jeyachandran, S., Baskaralingam, V., Thambusamy, S.: Improvement on dissolution rate of inclusion complex of Rifabutin drug with β-cyclodextrin. Int. J. Biol. Macromol. **62**, 472- 480 (2013)

11. Claudia, G., Ana, K.C., Marcela, L.: Improving furosemide polymorphs properties through supramolecular complexes of β-cyclodextrin. J. Pharm. Biomed. Anal. **95**, 139-145 (2014)

12. Yutaka, I., Noritaka I., Etsuo Y., Toshio, O., Kenjirou H., Kunikazu M., Keiji Y.: Solid states Fluorescence Study of *p*-Dimethylaminobenzonitorile by co-grinding with Cyclodextrins. Yakugaku Zasshi **129**, 253-262 (2009)

13. Erika, S., King, W.L., Madeleine, D., Florent, C., Kawthar, B.: Dehydration, Dissolution, and Melting of Cyclodextrin Crystals. J. Phys. Chem. B. **119**, 1433-1442 (2015)

14. Tarja, T., Teemu, H., Jukka, L., Laura, M., Sitaram, V., Pekka, J., Johan C., Vesa-Pekka, L., Tomi, J., Kristiina, J.: Crystal Structure Changes of γ-cyclodextrin After the SEDS Processing Supercritical Carbon Dioxide Affect the Dissolution Rate of Complexed Budesonide. Pharm. Res. **24**, 1058-1066 (2007)

15. Marcus, E.B., Thorsteinn, L.: Cyclodextrins as pharmaceutical solubilizers. Adv. Drug. Deliv. Rev. **59**, 645-666 (2007)

16. Lajos, S., Jozsef, S.: Cyclodextrins as food ingredients. Trends Food Sci. Tech. **15**, 137-142 (2004)

17. Ju, Y.F., Hui, L.C., Doryn, M.Y.T., Kim, T.T.: Bioavailability of tocotrienols: evidence in human studies. Nutr. Metab. **11**, 1-10 (2014)

18. Jianbin, C., Hongfang, W., Wei, Z., Min, Z., Liwei, Z.: Investigation of the inclusion behavior of chlorogenic acid with hydroxypropyl-β-cyclodextrin. Int. J. Biol. Macromol. **50,** 277- 282 (2012)

19. Kenjirou, H., Saori, I., Haruka, W., Kunikazu, M., Keiji, Y.: Incorporation of Salicylic Acid Molecules into the Intermolecular Spaces of γ-Cyclodextrin-Polypseudorotaxane.

Cryst. Growth Des. **9,** 4243-4246 (2009)

20. Zingone, G., Rubessa, F.: Preformulation study of the inclusion complex warfarin-β-cyclodextrin. Int. J. Pharm. **291**, 3-10 (2005)

21. Kenjirou, H., Saori, I., Haruka, W., Waree, L., Kunikazu, M., Keiji, Y.: Simultaneous Dissolution of Naproxen and Flurbiprofen from a Novel Ternary γ-Cyclodextrin Complex. Chem. Pharm. Bull. **58**, 769-772 (2010)

22. Yan, X., Hong, Y.P., Meng, X.Z., Xia, L., Wei, W.Z., Xiao, E.Y.: Caffeic acid product from the highly copper-tolerant plant *Elsholtzia splendens* post-phytoremediation: its extraction, purification, and identification. J. Zhejiang Univ. Sci. B. **13**, 487-493 (2012)

23. Samikannu, P., Krishnamurty, S., Meenakshisundaram, S., Rajaram, R.: Preparation and characterization of host–guest system between inosine and b-cyclodextrin through inclusion mode. Spectrochim Acta. A. Mol. Biomol. Spectrosc. **147**, 151-157 (2015)

418 Figure Legend

419 Fig. 1 Chemical structure.

420 (a) Caffeic acid (CA), (b-1) γ-Cyclodextrin (γ-CD), (b-2) D-glucopyranose

421 Fig. 2 PXRD patterns of CA/γ-CD mixtures.

422 (a) CA crystals, (b) CA ground for 60 min, (c) freeze-dried CA, (d) γ-CD, (e) freeze-dried

423 γ-CD, (f) γ-CD ground for 60 min,

424 (g) PM (CA/γ-CD=1/1), (h) CP, (i) FD (CA/γ-CD=1/1), (j) GM 60 min (CA/γ-CD=1/1)

425 Fig. 3 DSC curves produced by CA/γ-CD mixtures.

426 (a) CA, (b) γ-CD, (c) PM (CA/γ-CD=1/1), (d) CP, (e) FD (CA/γ-CD=1/1), (f) GM

427 (CA/γ-CD=1/1)

428 Fig. 4 FT-IR spectra produced by CA/γ-CD mixtures.

429 (a) CA, (b) γ-CD, (c) PM (CA/γ-CD=1/1), (d) CP, (e) FD (CA/γ-CD=1/1), (f) GM

430 (CA/γ-CD=1/1)

431 Fig. 5 SEM photographs of CA/γ-CD mixtures.

432 (a) CA, (b) freeze-dried CA, (c) ground CA, (d) γ-CD, (e) freeze-dried γ-CD, (f) ground γ-CD,

433 (g) PM (CA/γ-CD=1/1), (h) CP, (i) FD (CA/γ-CD=1/1), (j) GM (CA/γ-CD=1/1)

434 Fig. 6 Integral strength of the CP according to ^{1}H-NMR measurement.

435 Fig. 7 ^{1}H-^{1}H NOESY NMR spectrum produced by the CP (molar ratio of CA/γ-CD=1/1) in

436 D_2O. (a) X is 5.7-7.3 and Y is 3.3-3.9.

437 ^{1}H-^{1}H NOESY NMR spectrum produced by the FD (molar ratio of CA/γ-CD=1/1) D_2O. (b)

438 X is 5.7-7.4 and Y is 3.3-3.9.

439 ^{1}H-^{1}H NOESY NMR spectrum produced by the GM (molar ratio of CA/γ-CD=1/1) D_2O. (b)

440 X is 6.0-7.5 and Y is 3.3-4.0.

441 Fig. 8 Dissolution profiles of CA/γ-CD mixtures Results are presented as the mean ± S.D.

442 (n=3).

443 Fig. 9 DPPH radical scavenging test of CA/γ-CD mixtures Results are presented as the

444 mean ± S.D. (n=3).

445 (a) CA, (b) PM (CA/γ-CD=1/1), (c) CP, (d) FD (CA/γ-CD=1/1), (e) GM (CA/γ-CD=1/1), (f)

446 AA, (g) γ-CD

447 Fig. 10 IC_{50} of CA/γ-CD mixtures in the DPPH radical scavenging test Results are

448 presented as the mean ± S.D. (n=3).

449 * : $p<0.05$ vs. AA, ** : $p<0.01$ vs. AA (*Tukey Kramer test*)

450

451 Diagram. 1 Structural view of a CA/γ-CD complex.

452

a)

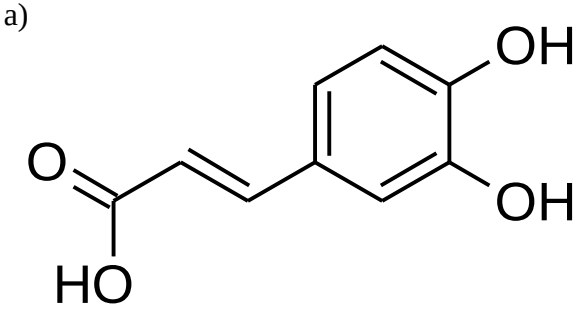

b-1)

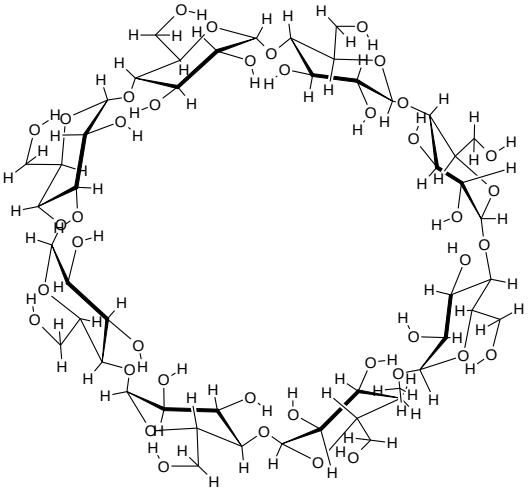

b-2)

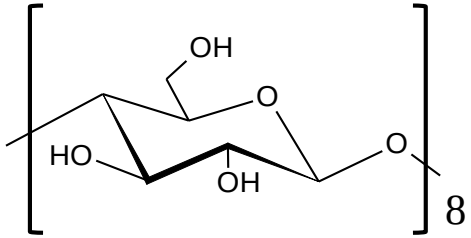

Fig. 1 Chemical structure.
(a) Caffeic acid (CA) ,(b-1) γ-Cyclodextrin (γ-CD), (b-2) D-glucopyranose

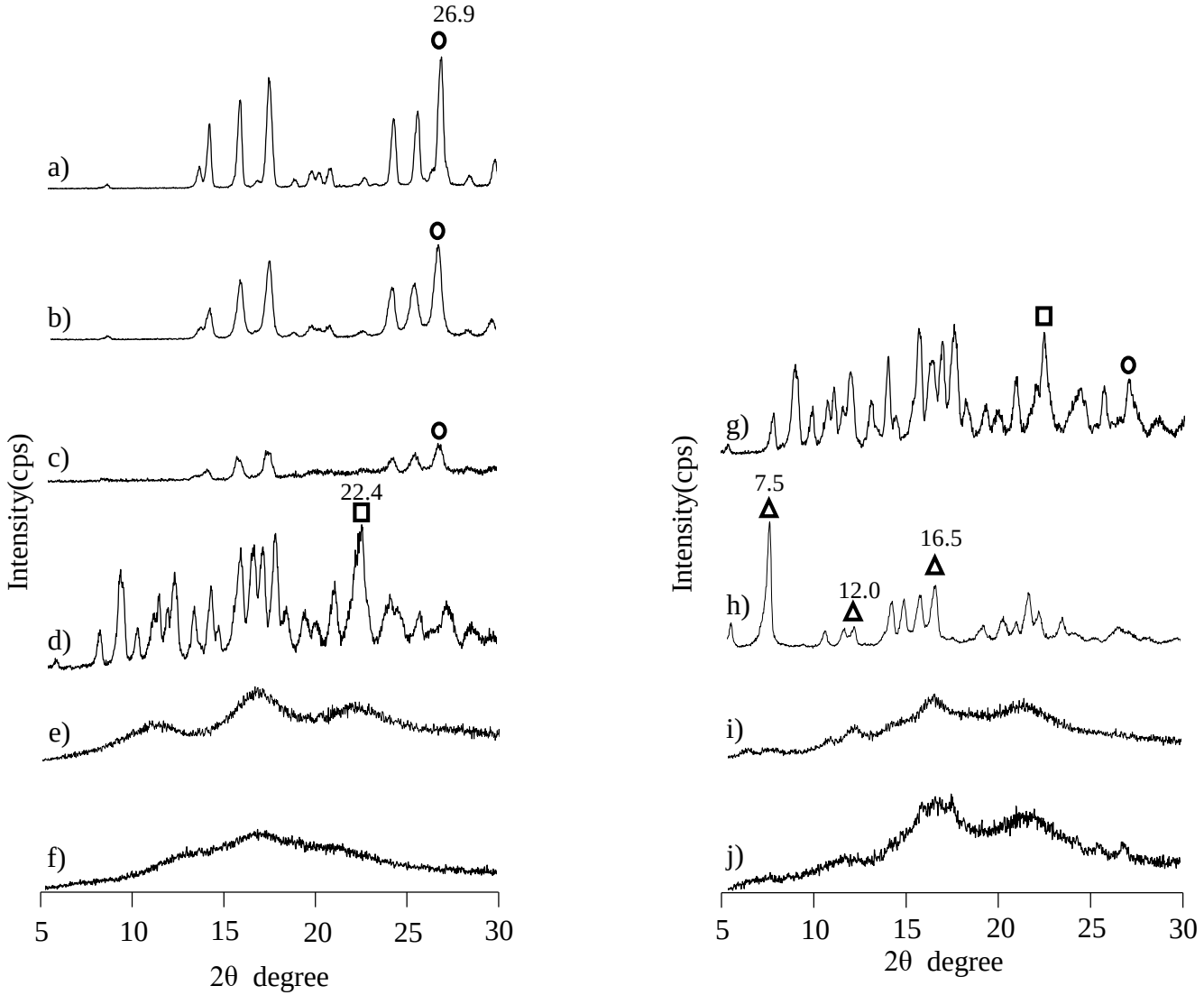

Fig. 2 PXRD patterns of CA/γ-CD mixtures.
(a) CA, (b) CA ground for 60 min, (c) freeze-dried CA, (d) γ-CD, (e) freeze-dried γ-CD, (f) γ-CD ground for 60 min, (g) PM (CA/γ-CD=1/1), (h) CP, (i) FD (CA/γ-CD=1/1), (j) GM 60 min (CA/γ-CD=1/1)

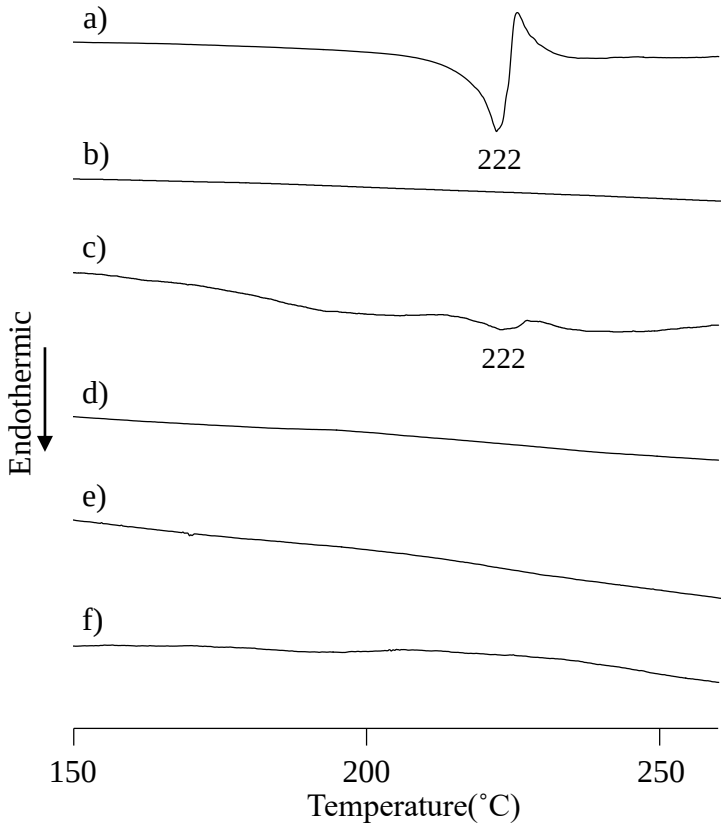

Fig. 3 DSC curves produced by CA/γ-CD mixtures.
(a) CA, (b) γ-CD, (c) PM (CA/γ-CD=1/1), (d) CP, (e) FD (CA/γ-CD=1/1), (f) GM (CA/γ-CD=1/1)

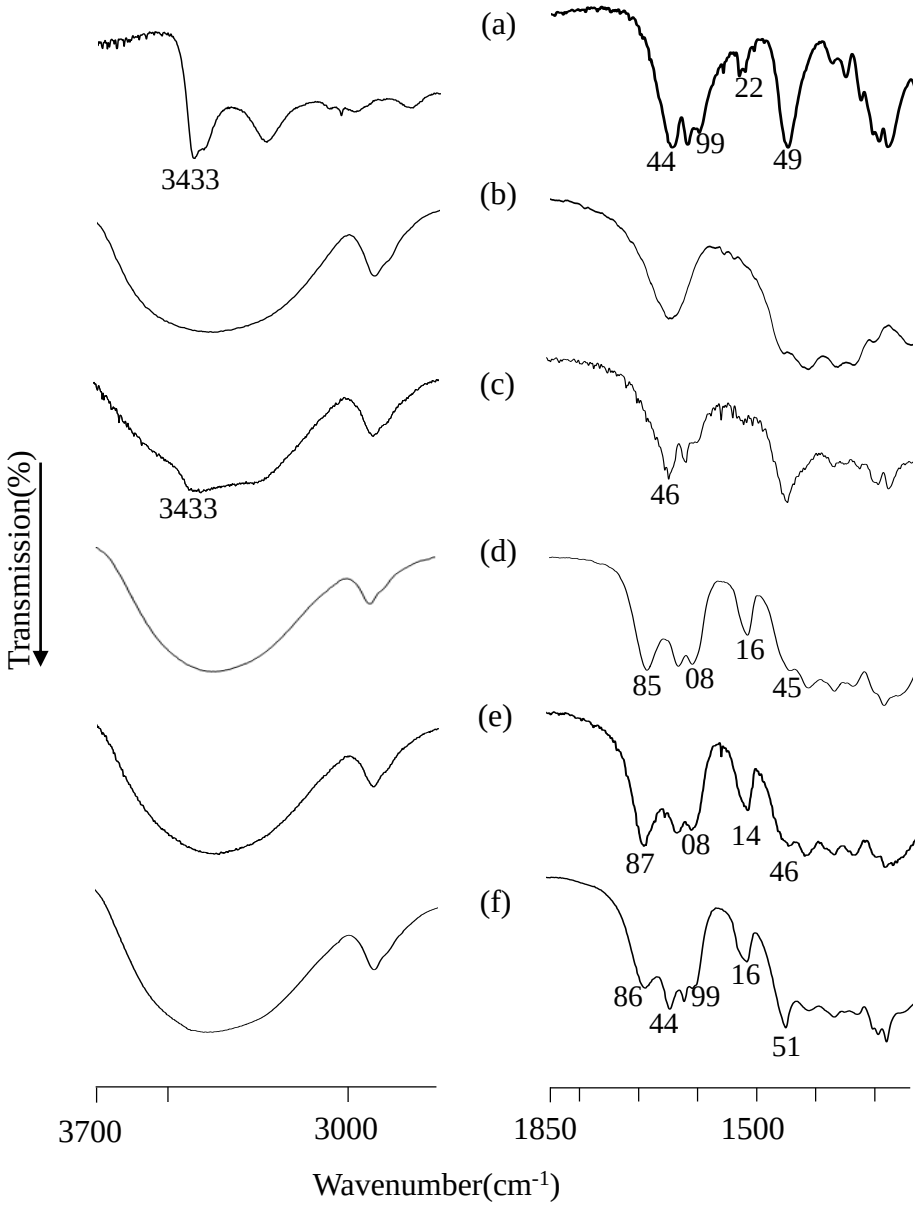

Fig. 4 FT-IR spectra produced by CA/γ-CD mixtures.
(a) CA, (b) γ-CD, (c) PM (CA/γ-CD=1/1), (d) CP, (e) FD (CA/γ-CD=1/1), (f) GM (CA/γ-CD=1/1)

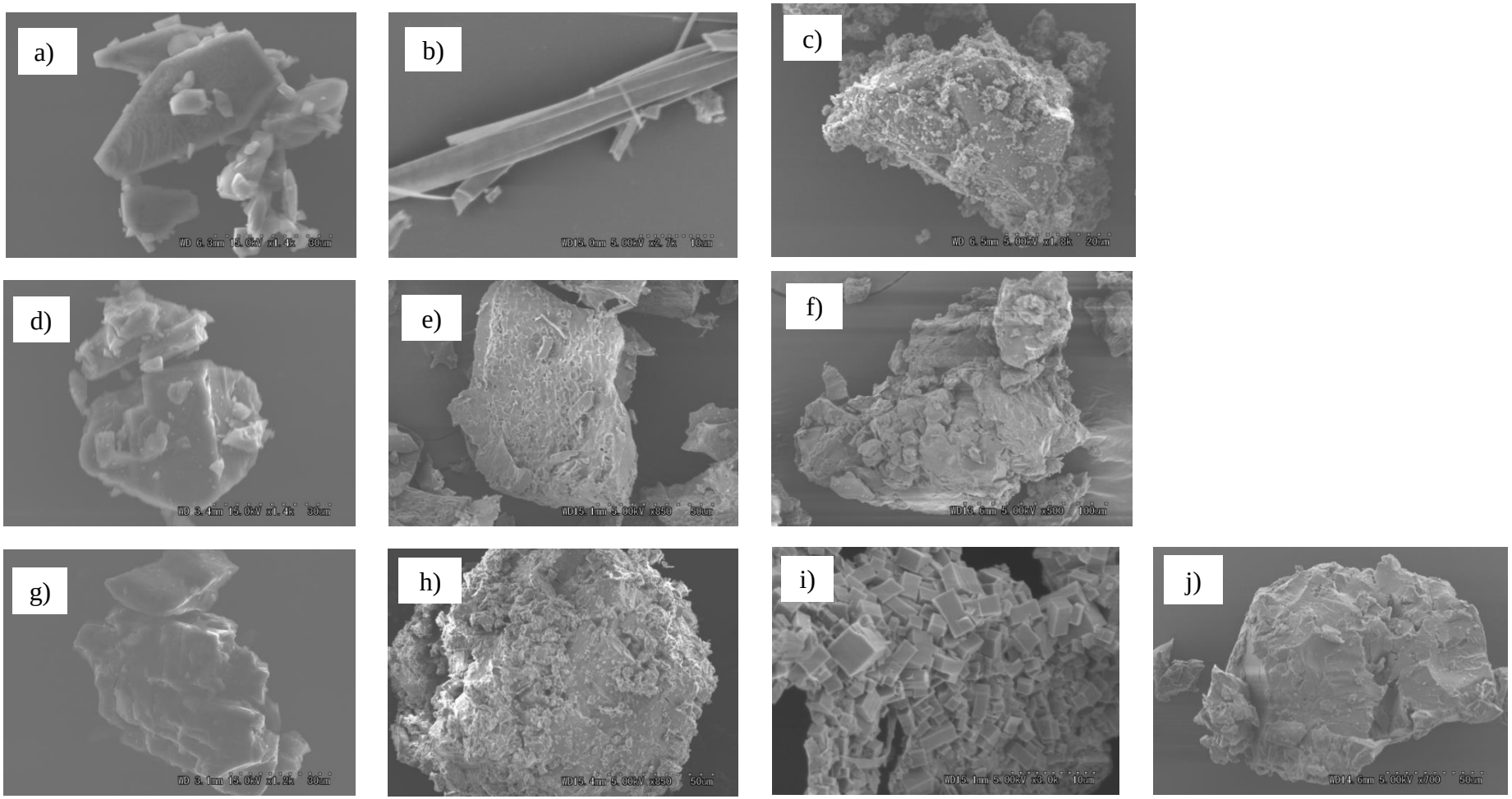

Fig. 5 SEM photographs of CA/γ-CD mixtures.
(a) CA, (b) freeze-dried CA, (c) CA ground for 60 min, (d) γ-CD, (e) freeze-dried γ-CD, (f) γ-CD ground for 60 min, (g) PM (CA/γ-CD=1/1), (h) CP, (i) FD (CA/γ-CD=1/1), (j) GM (CA/γ-CD=1/1)

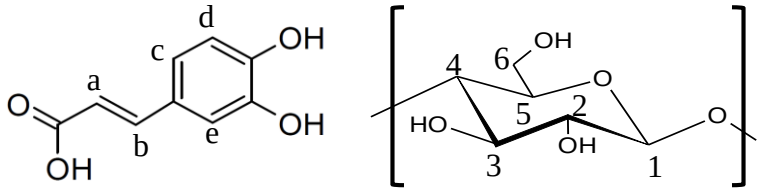

a)

The number of molecules of γ-CD to a molecule of CA
9.44 / 8 = 1.18

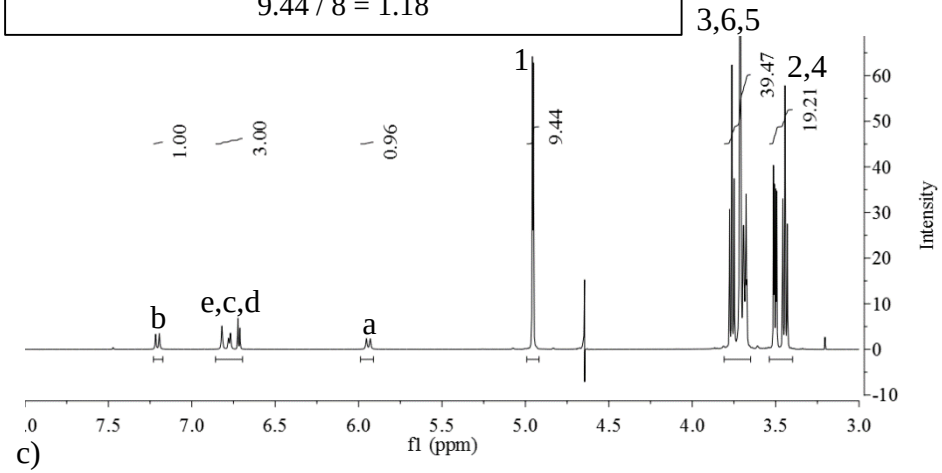

b)

The number of molecules of γ-CD to a molecule of CA
6.98 / 8 = 0.87

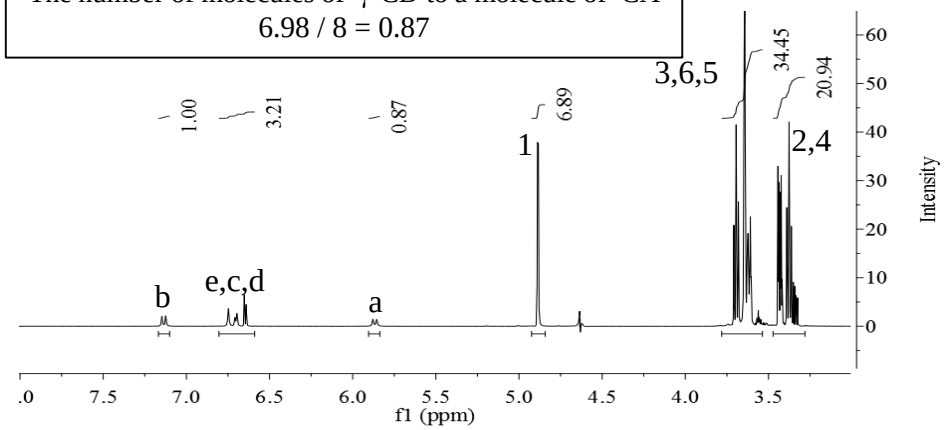

c)

The number of molecules of γ-CD to a molecule of CA
8.59 / 8 = 1.07

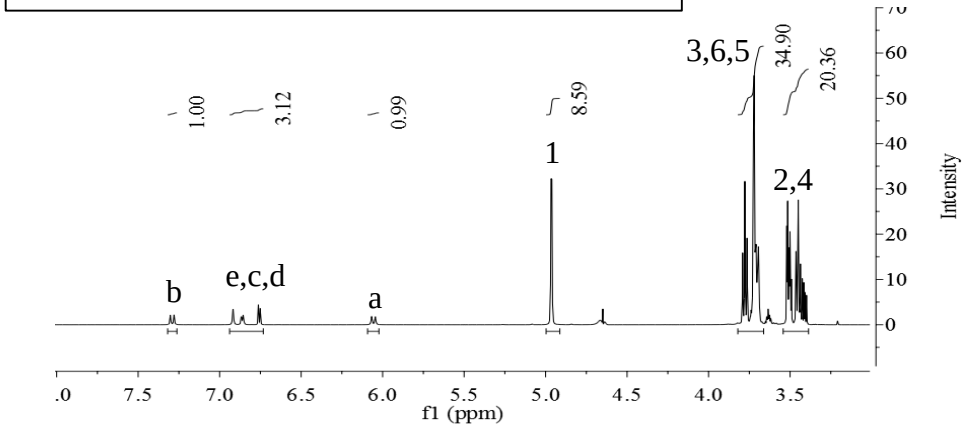

Fig. 6 Integral strength of CA/γ-CD mixtures according to ^{1}H-NMR measurement.
(a) CP, (b) FD (CA/γ-CD=1/1), (c) GM (CA/γ-CD=1/1)

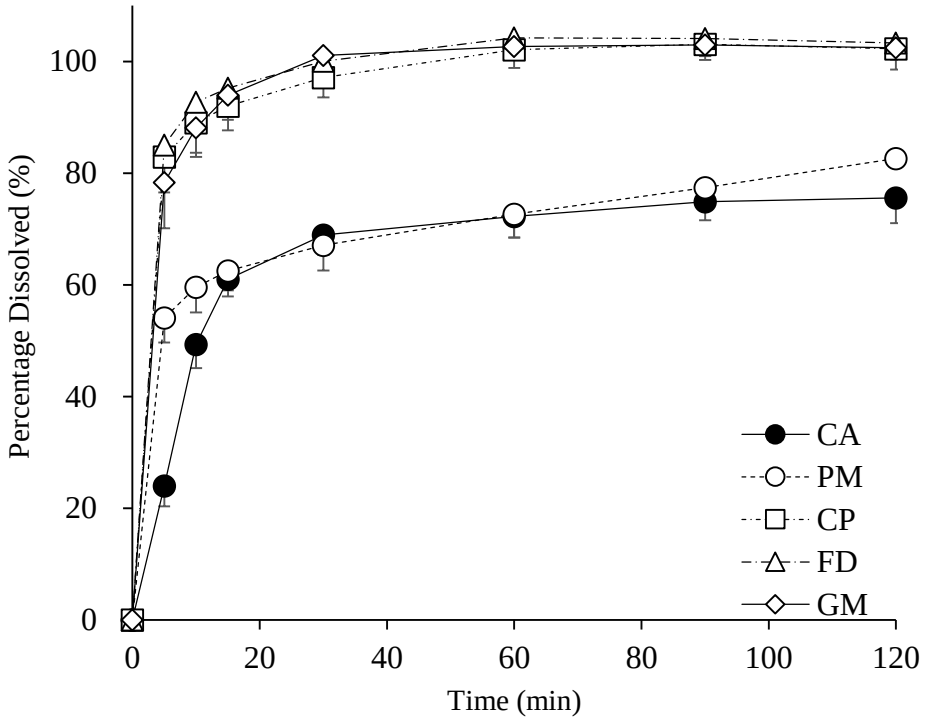

Fig. 8 Dissolution profiles of CA/γ-CD mixtures, Results are presented as the mean ± S.D. (n=3).

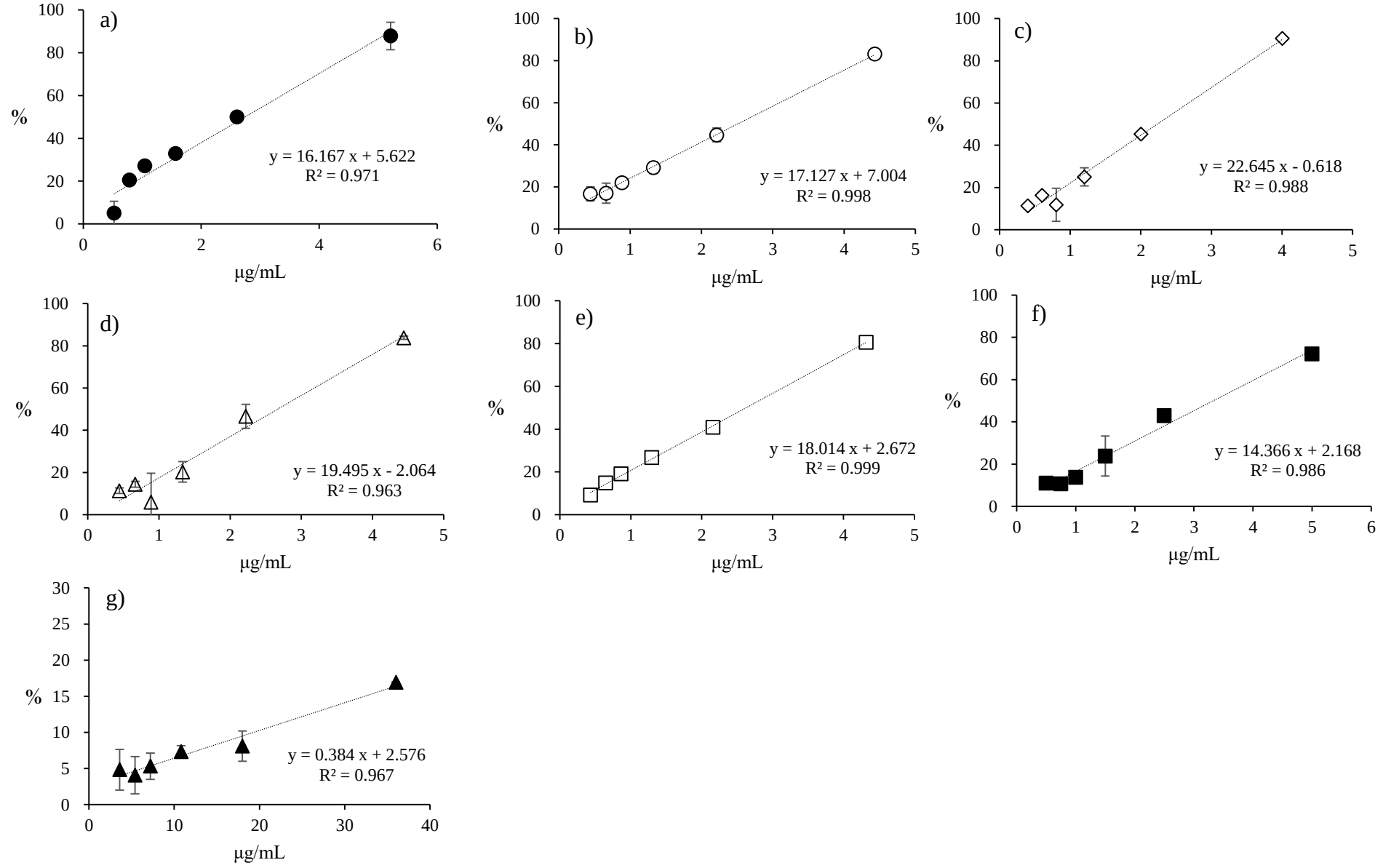

Fig. 9 DPPH radical scavenging test of CA/γ-CD mixtures, Results are presented as the mean ± S.D. (n=3).
(a) CA, (b) PM (CA/γ-CD=1/1), (c) CP, (d) FD (CA/γ-CD=1/1), (e) GM (CA/γ-CD=1/1), (f) AA, (g) γ-CD

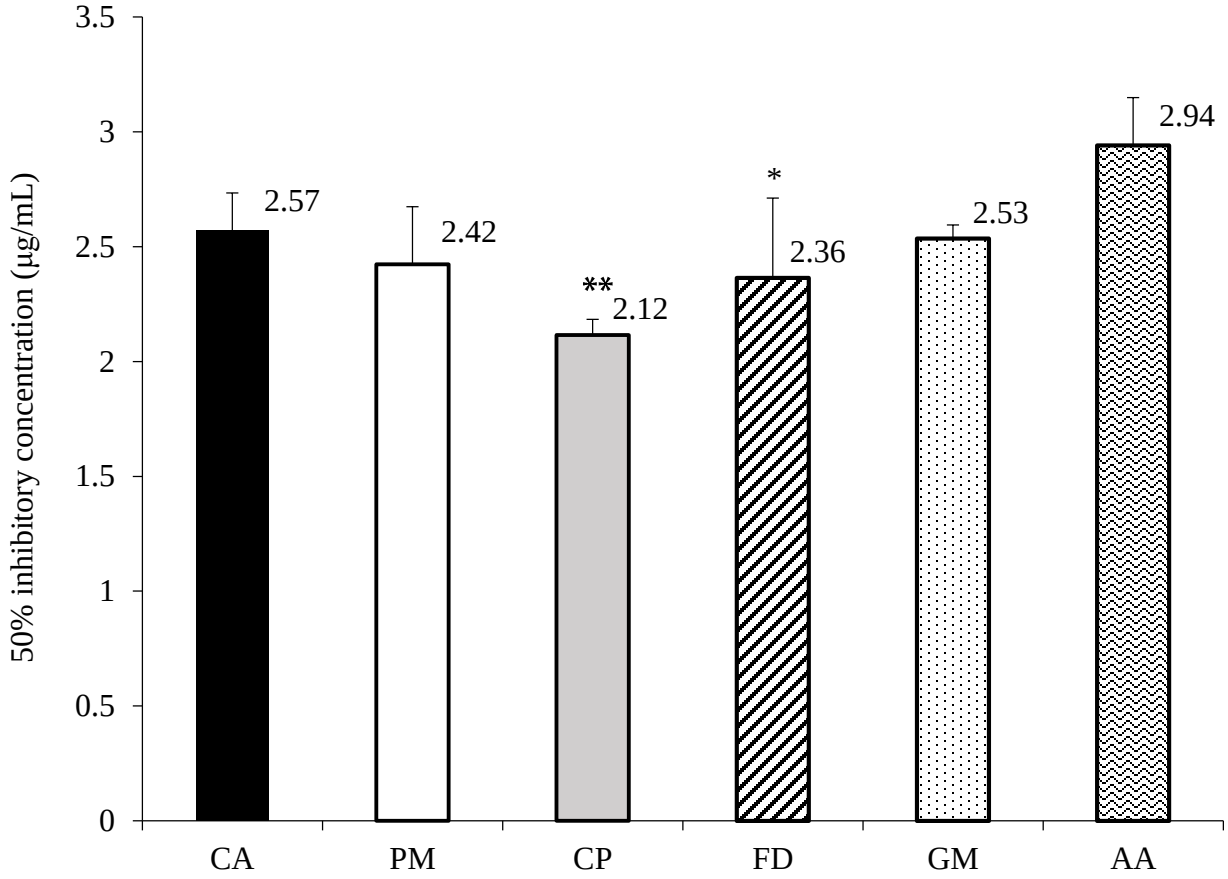

Fig. 10 IC_{50} of CA/γ-CD mixtures in the DPPH radical scavenging test, Results are presented as the mean ± S.D. (n=3). *: $p<0.05$ vs. AA, **: $p<0.01$ vs. AA (*Tukey Kramer test*)

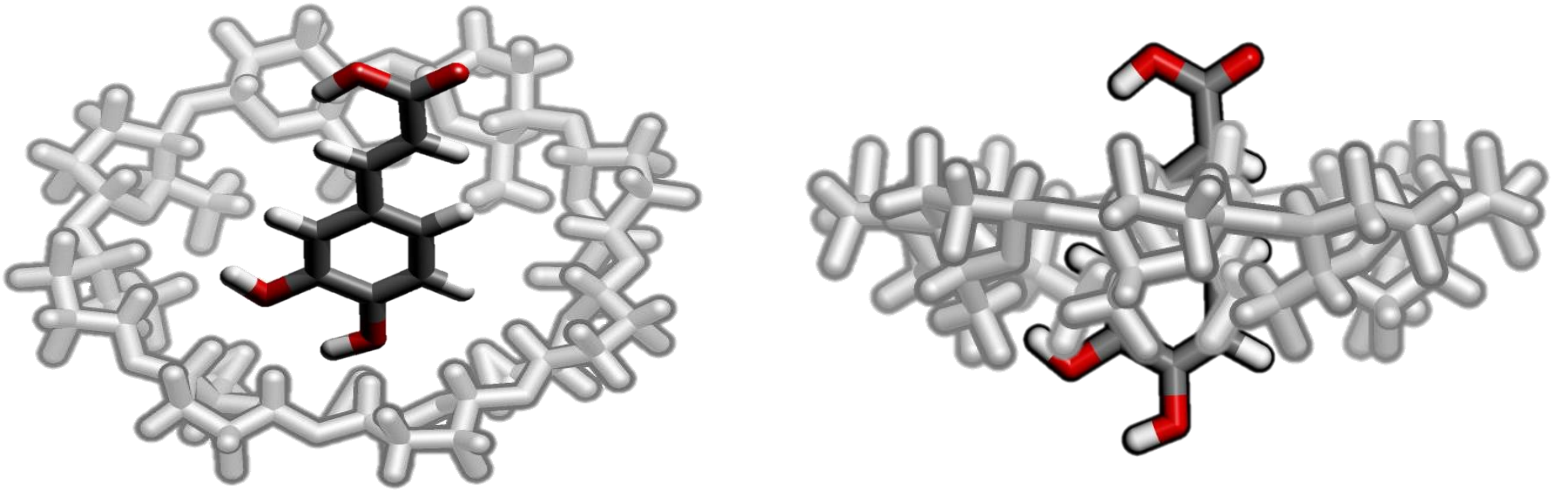

Diagram. 1 Structural view of a CA/γ-CD complex.